AMBIENT USE-CONDITION MODELS FOR RELIABILITY ASSESSMENT

Chen Gu, Robert F. Kwasnick, Neal R. Mielke, Eric M. Monroe, C. Glenn Shirley*

Intel Corporation
*5200 NE Elam Young Parkway MS: RA1-329
Hillsboro, Oregon 97124 USA

ABSTRACT

We describe methods of computing reliability acceleration for realistic temperature/humidity use-condition models. We extract outdoor temperature/humidity models based on NOAA [1] data, and indoor and automotive interior models by using the NOAA data combined with additional data which characterizes thermal and human behavior (thermostat settings). We compare predictions of these models with traditional reliability assessments, and provide useful models to represent the results.

INTRODUCTION

Reliability assessment of a population of units of an electronic component depends on a model of the failure mechanisms, which includes models of acceleration and lifetime statistics, and on a model of the "use condition". Much work has been done to derive accurate models for different failure mechanisms, but little has been published on the use conditions to which those reliability models should be extrapolated. The use condition assumed is often a steady-state ambient set to be worse than all ambients. This approach is easy, but may be too conservative, forcing unnecessary constraints on technologies, designs, etc. As a result, there is increased interest in knowledge-based reliability assessment [2] which combines models for reliability models and use conditions.

This paper shows how to compute acceleration factors from use-condition data. Part of the "use-condition" is the temperature-humidity (T_{air}/h_{air}) of the ambient air surrounding the electronic equipment in which the component is installed, and another part is the temperature rise (T_{rise}) at the device due to local heating. We generate models for outdoor and indoor temperature-humidity use conditions, and for vehicle-interior temperature use conditions. We then calculate the statistics of reliability acceleration for the Arrhenius/Peck [3,4] moisture reliability acceleration model in each of these environments, for a range of activation energies and humidity-related acceleration parameters. Then we express the results of these calculations as useful regression models. Finally, we show how to take arbitrary models of T_{rise} into account, although we don't consider any specific (except trivial) models.

AF FOR TIME-VARYING USE CONDITIONS

The parameter which relates laboratory-derived reliability models to "use conditions" is the acceleration factor (AF) of the use condition relative to a "reference" condition which is defined as

$$AF_{eff}(use \mid ref) = \frac{t_{ref}}{t_{use}} = \frac{MTTF_{ref}}{MTTF_{use}} \tag{1}$$

where the right hand side of (1) is the ratio of the time at the reference condition to the time in "use" for which the same "effect" is observed. The effect might be a particular percentile of the population failing. One particular case of this is the mean time to failure (MTTF).

For the usual treatment of use-conditions, the acceleration in Eq. (1) would be computed by substituting constant values of use-condition environmental variables into a formula for the acceleration. However, when the use-condition varies with time, the more general expression for the effective acceleration is:

$$AF_{eff}(use \mid ref) = \frac{1}{t_{use}} \int_0^{t_{use}} AF\left[use \mid ref,\, T_{use}(t),\, h_{use}(t)\right] dt \tag{2}$$

where we specialize to the case of temperature-humidity acceleration, and show the time variation through the time variation of the "use" temperature, T_{use} , and humidity, h_{use}.

It is unnecessary (and impractical) to do this integration directly because a simpler statistical method is available. The key is to recognize the equivalence of Eq. (2) and the following:

$$\begin{aligned} AF_{eff}(use \mid ref) &= \langle AF(use \mid ref; T, h) \rangle \\ &\equiv \int_0^{\infty} dT \left[\int_0^{1} dh \cdot \rho(T,h) \cdot AF(use \mid ref, T, h) \right] \end{aligned} \tag{3}$$

where $\rho(T,h)$ is a joint probability density function (PDF) of temperature and humidity, and $\langle\ \rangle$ denotes a time average. Eqs (2) and (3) may be understood to be equivalent by the following argument: As time t increases, the environmental condition, expressed as a point in (T_{use}, h_{use})-space, traces out a trajectory. Because environmental conditions are quasi-cyclical (revisiting the same region many times), this trajectory will define a density function $\rho(T,h)$ in this space. Notice that this equivalence is possible because, in this model, the *sequence* of environmental conditions does not affect the accumulation of degradation – it is merely the fraction of the overall use time spent at each distinct condition which matters. Also, Eqs. (2) and (3) assume that the temperature at the point of action of the reliability mechanism tracks the externally applied temperature profile – a quasi static assumption. This is valid for slow (eg. diurnal) temperature variation and small device thermal mass. Mathematically, Eq. (3) is the expectation value, $\langle\rangle$, of the acceleration function taken over the joint probability distribution in time of the temperature and humidity.

In Eq. (2), T_{use} and h_{use} are defined as the temperature and humidity at the point of action of the mechanism in the device. We assume a model in which $T_{use}(t)$ is the time-varying ambient temperature $T_{air}(t)$ offset by a local time-varying temperature rise, $T_{rise}(t)$, uncorrelated in time. So,

$$T_{use}(t) = T_{rise}(t) + T_{air}(t) \tag{4}$$

and Eq. (3) becomes

$$AF_{eff}(use \mid ref) = \int_0^\infty dx \cdot \kappa(x) \left\{ \int_0^\infty dy \cdot \lambda(y) \left[\int_0^1 dz \cdot \mu(z,y) \cdot AF(use \mid ref; x, y, z) \right] \right\} \quad (5)$$

where, for compactness, we associate

$$T_{rise} \to x\,,\ T_{air} \to y\,,\ h_{air} \to z\,.$$

and where we have factorized the PDF as follows:

$$\rho(x,y,z) = \kappa(x)\lambda(y)\mu(y,z) \quad (6)$$

This factorization has used the assumption that T_{rise} and T_{air} are uncorrelated in time. The factorization of the ambient air PDF into the two functions, $\lambda(T_{air})$ and $\mu(T_{air}, h_{air})$ is made for convenience, and no further loss of generality occurs by doing this. If the function μ were independent of T_{air} then temperature and relative humidity would also be uncorrelated, but we are not assuming this.

The Arrhenius/Peck temperature/humidity acceleration model in Eq. (5), taking into account the effect of T_{rise}, is written:

$$AF(use \mid ref; x, y, z) = \left(\frac{P_{sat}(y)}{P_{sat}(x+y)} \right)^C \left(\frac{z}{h_{ref}} \right)^C \exp\left\{ \frac{Q}{k_B} \left(\frac{1}{T_{ref}} - \frac{1}{x+y} \right) \right\} \quad (7)$$

where $P_{sat}(T)$ is the saturated vapor pressure of water vapor. This assumes that the partial pressure of water vapor at the point of action of the mechanism is the same as in the surrounding ambient, which is an ideally non-hermetic case (quasi-static with respect to moisture diffusion). A fitted formula for $P_{sat}(T)$ is available [5]. If we use the leading order approximation

$$P_{sat}(T) = P_0 \exp\left(-\frac{W}{k_B T} \right) \quad (8)$$

where W is the latent heat of vaporization of water (0.42 eV), then Eq. (7) becomes

$$AF(use \mid ref; x, y, z) = \left(\frac{z}{h_{ref}} \right)^C \exp\left\{ \frac{Q}{k_B} \left(\frac{1}{T_{ref}} - \frac{1}{x} \right) \right\} \exp\left\{ \frac{(Q - WC)}{k_B} \left(\frac{1}{x} - \frac{1}{x+y} \right) \right\} \quad (9)$$

Since T_{rise} is always small compared to T_{air} when measured in ºK it is often a good approximation to write

$$AF(use \mid ref; x, y, z) \cong \left(\frac{z}{h_{ref}} \right)^C \exp\left\{ \frac{Q}{k_B} \left(\frac{1}{T_{ref}} - \frac{1}{y} \right) \right\} \exp\left\{ \frac{(Q - WC)x}{k_B y^2} \right\} \quad (10)$$

Parametric forms for the distributions κ, λ, and μ were defined as given in the Appendix. Because the environmental PDF in Eq. (6) is defined at each of many locations, the parameters of each of these distributions will be a function of location. Numerical integration of Eq. (5) using the parametric forms for κ, λ, and μ and the AF model of Eq. (7) was done using the method given in the Appendix.

EXTRACTION OF USE CONDITION PARAMETERS

We describe in this section how a very large amount of climatic data was distilled into a manageable dataset of use-condition model parameters defining the PDFs $\lambda(y)$, and $\mu(y,z)$ as in the Appendix, while preserving accuracy sufficient for reliability calculations.

We do not have a specific model for the T_{rise} PDF, $\kappa(x)$, to consider in this paper, so we did model calculations assuming that $\kappa(x)$ is a delta function in time (T_{rise} is constant in time) at each location. Later, we will show how to relax this assumption.

For the climatic data, we purchased hourly data from the National Oceanographic and Atmospheric Administration (NOAA) weather database [1]. NOAA monitors 26 dynamic climatic weather datums including temperature (dry bulb and wet bulb), wind velocity, cloud cover, etc. and provides static data on state, country, altitude, latitude, and longitude. Data is reported by city and is grouped by country. The data spanned more than 1400 weather stations worldwide, except Antarctica. NOAA collected data evenly throughout the day every one to three hours from 1982 through 1997. The NOAA database therefore provides for each of the 1400 locations a temperature/humidity time series which could, in principle, be directly integrated in Eq. (2). In practise this is unfeasible because of the large size of the time-series dataset (260 GB). However, the density function formulation described above makes it possible to distill this dataset into a compact set of location-specific CDFs, manageable in Excel, from which distribution parameters described in the Appendix can be extracted.

Outdoor Environment

As an example of the outdoor environment, we show the fit of NOAA climate data for one of the 1441 stations, Phoenix, to the model Eq. (A3) in Fig. 1 (top) and Eq. (A6) in Fig. 1 (bottom). This is a fit of the cumulative density function (CDF) of daily average data, which does not include the within-day variation. Systems exposed directly to outdoor ambients will also be subjected to diurnal (day/night) temperature variation, so the variances in the final model parameters were modified slightly to take this into account as follows:

$$T_{\text{var1}} \leftarrow T_{\text{var1}} + T_{\text{diurnal\_variance}} \qquad T_{\text{var2}} \leftarrow T_{\text{var2}} + T_{\text{diurnal\_variance}}$$

It is apparent from Fig. 1 that a bimodal distribution fits the temperature CDF of Phoenix well, whereas a simple normal distribution would not be a good fit, and the humidity distribution varies with temperature. Phoenix was one of 1441 stations for which distribution parameters were extracted. Although some stations did not require as many parameters as shown in Fig. 1, the parameterization in Fig. 1 was sufficient for all stations.

Indoor Environment

The indoor environment is important, since this is the "climate" where most electronic equipment is used. An empirical study was performed, in a hot climate, to determine how to estimate indoor temperature data from the outdoor data available in the NOAA database. For twelve weeks in the summer of 2000 forty students from St. Stephen's College in New Delhi, India measured the temperature inside and outside their non-air-conditioned homes four times daily (at mid-morning, early afternoon, early evening, and late evening). Results indicated that home thermal-mass effects caused indoor temperature to lag outdoor temperature changes, similar to the effect of a low-pass filter in electronics. Indoor temperatures were

stable enough from hour to hour that only the average for the day was needed to accurately estimate reliability impact. We see in Fig. 2 that this daily average T_{air_indoor} could be accurately predicted from the outdoor average temperature, T_{air} , for the day in question ("n"), and the previous two days ("n-1" and "n-2"):

$$T_{air\_indoor}(n) = 11.1 + 0.648 \times \left[0.54 \times T_{air}(n) + 0.28 \times T_{air}(n-1) + 0.18 \times T_{air}(n-2)\right] \quad (11)$$

where temperatures are in °C and the term in brackets is a weighted three-day average of the outdoor temperature. This formula was checked for one additional home, in Northern California in November 2000 and found accurate to 1 °C (Fig. 2). We extended this by computing the corresponding indoor RH as:

$$h_{indoor}(n) = h_{air}(n) \frac{P_{sat}\left[T_{air}(n)\right]}{P_{sat}\left[T_{air\_indoor}(n)\right]}. \quad (12)$$

The model fitted for one of 1367 stations, Phoenix, is shown in Fig. 3, which may be compared to Fig. 1. Note that this model is for uncontrolled indoor environments, so that a model for a controlled indoor environment would also include values for heating and cooling limits, T_{min} and T_{max}. Models for these limits, which may vary from location to location might, for example, be obtained by surveys of building thermostat settings. Since we did not have this data, we chose a reasonable heating limit of T_{min} = 22.2 °C for every location to represent the "Indoor Controlled" environment.

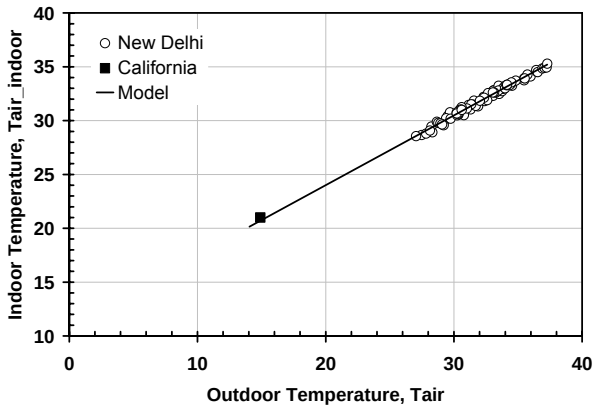

FIG. 2. INDOOR VS. OUTDOOR AMBIENT TEMPERATURE. INDOOR DAILY-AVERAGE TEMPERATURE FOR EACH HOME IS LINEARLY RELATED TO A THREE-DAY WEIGHTED AVERAGE OF THE OUTDOOR TEMPERATURE.

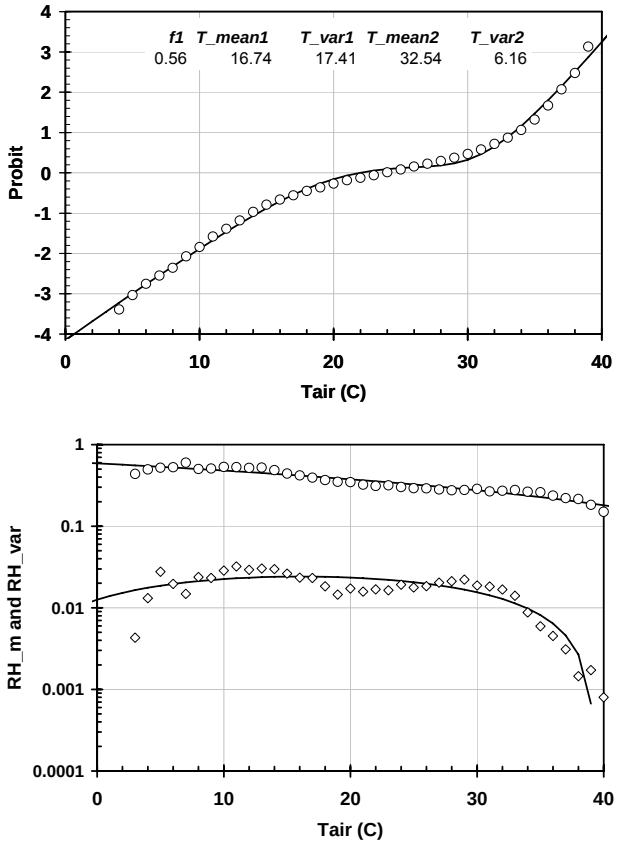

FIG. 1. OUTDOOR ENVIRONMENT IN PHOENIX, ARIZONA (NOAA STATION 722780). TOP: CDF PLOTS OF NOAA DATA OF DAILY TEMPERATURES AND FITTED DISTRIBUTION, EQ. (A3). BOTTOM: HUMIDITY DISTRIBUTION PARAMETERS, EQS. (A6), FOR EACH VALUE OF T_{AIR}.

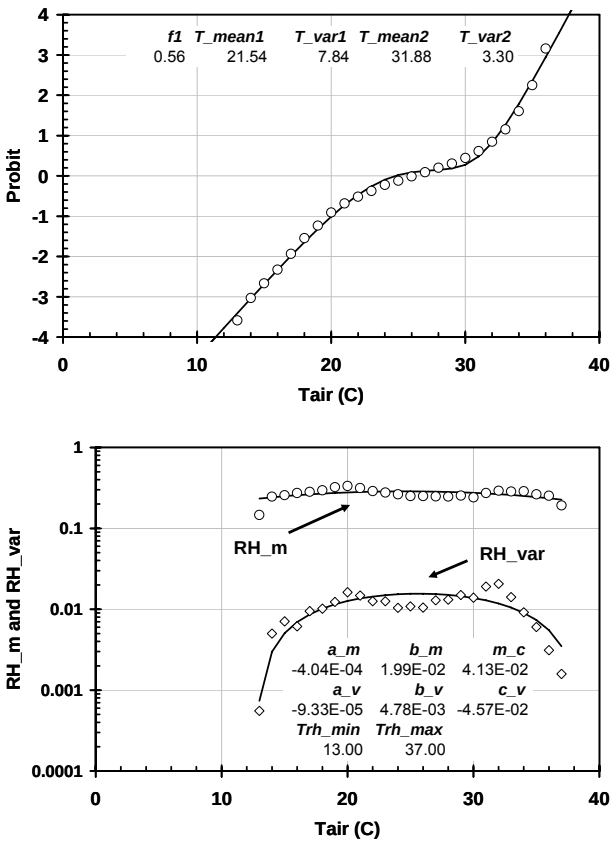

FIG. 3. INDOOR UNCONTROLLED ENVIRONMENT IN PHOENIX, (NOAA STATION 722780). TOP: CDF PLOTS OF DAILY TEMPERATURES AND FITTED DISTRIBUTION, EQ. (A1). BOTTOM: HUMIDITY DISTRIBUTION PARAMETER, EQS. (A6), VS T_{AIR}.

Vehicle Dashboard Temperature Environment

Portable electronic devices are often placed in the interiors of motor vehicles, which can become hot when parked and unoccupied, especially when exposed to solar radiation on sunny days. We develop a model of solar heating of directly exposed dashboard surface inside a car. The model does not consider scenarios in which users may place a device in a location not directly exposed to solar radiation. The dashboard surface is generally the hottest location for a portable electronic device in a car.

We measured dashboard temperature with small temperature sensors [6] at 7 geographical locations between 21° and 43° north latitude in 21 closed cars of different sizes and colors over 16 different days between February and November, 2004. The observers were asked to position their cars south-facing on a sunny day, put sensors on the dashboard and under the vehicle (to measure T_{air}), close the windows, and take data during daylight hours. Fig. 7 shows the results for one location, and a model fit.

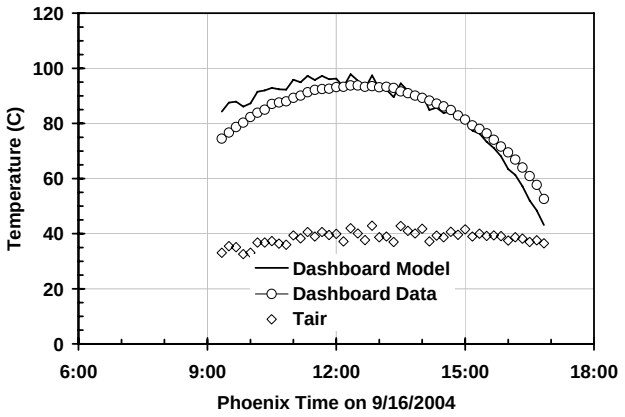

FIG. 7 EXTERNAL AIR TEMPERATURE, DASHBOARD TEMPERATURE AND MODEL FIT DURING ONE SUNNY DAY IN PHOENIX, AZ.

The temperature of components in a device on a dashboard, T_{dash}, depends on the air temperature external to the vehicle, T_{air}, a contribution due to the solar energy impinging on the dashboard, T_{solar}, and a contribution from heating of the air in the enclosed vehicle. We model the local temperature rise on the dashboard above the ambient temperature external to the car as entirely due to direct solar radiation. Although this ignores the temperature rise of air inside the vehicle, it covers the main effect, and we expect that the effect of interior air temperature rise will be absorbed into some of the parameters of the solar model when fitted to data. We also ignore the local self-heating temperature rise, T_{rise}, inside any device that may be running. For portable devices, this is expected to be negligible compared to the solar-induced temperature rise of 50 – 60 ºC (Figs. 7 and 8). So we write

$$T_{dash} = T_{air} + T_{solar} \tag{13}$$

where T_{air} comes from the NOAA database [1], and the solar component is expressed as [7]

$$T_{solar} = M_{dash} \times DF \times CF \tag{14}$$

where

$$DF = \tau^{\frac{1}{\cos\theta_{sun}}} \times \cos\left[\arcsin\left(\frac{\sin\theta_{sun}}{n}\right)\right] \tag{15}$$

and where

$$CF = 1 - F_{cloud}/11.5 \tag{16}$$

In Eq. (14), M_{dash} is a constant representing the maximum temperature rise due to solar exposure, DF is a derating factor depending on the angle of the sun measured from the zenith, θ_{sun}, at a particular latitude and time of day, and CF is a derating factor for a reduction in radiation due to average cloud cover. In the expression for DF, the term involving τ gives the optical transmittance of the atmosphere (0.7 corresponds to a clear day), and n is the effective refractive index of the atmosphere. In the expression for CF, the value of F_{cloud} is obtained from the "Total Sky Coverage" parameter in the NOAA database. $F_{cloud} = 0$ corresponds to no cloud coverage, and $F_{cloud} = 10$ corresponds to complete cloud coverage.

We fitted the model of Eqs. (13-16) to the data using M_{dash} and n as fitting parameters. Fig. 8 shows the actual vs. predicted daily maximum temperature for each car. In Fig. 8, the actual maximum temperatures tend to be cooler than predicted because the model values (x-axis) were computed with F_{cloud} set to 0. Although the data were taken on substantially sunny days, in some locations there was non-zero cloud cover, which reduced the actual daily maximum temperature (y-axis).

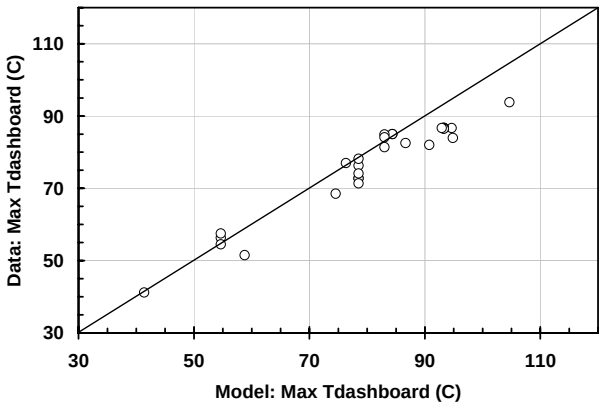

FIG. 8 DASHBOARD MAXIMUM DAILY TEMPERATURE MODEL VERSUS DATA FOR 21 VEHICLES OVER 16 DAYS IN 7 LOCATIONS AROUND THE WORLD.

DISCUSSION

In Fig. 9 we show correlation plots of the time-average temperature and time-average humidity at each of many locations for the outdoor environment. While the time-averages of environment in Fig. 9 give a good idea of the climate, they are not, in general, sufficient to compute the AFs. Computation of AFs requires averaging the AF over the correlated temperature humidity profiles using the methods described above. To quantify this, we compare the following AF estimators:

$$AF_{at\ mean}(use \mid ref) = AF\left(use \mid ref; x = 0, \langle y \rangle, \langle z \rangle\right) \tag{17a}$$

$$AF_{eff}(use \mid ref) = \langle AF\left(use \mid ref; x = 0, y, z\right) \rangle \tag{17b}$$

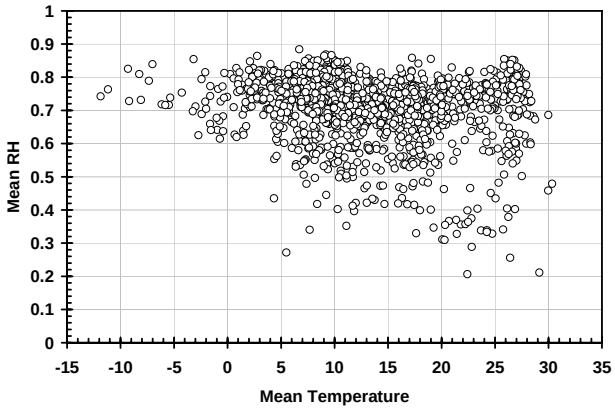

FIG. 9 TIME-AVERAGE RELATIVE HUMIDITY VS TIME-AVERAGE TEMPERATURE FOR OUTDOOR ENVIRONMENT.

Fig. 10 shows this comparison for a reference condition of 25/85 and for a Peck acceleration model with Q = 0.9 eV, and C = 3. We chose this acceleration model because it has been recommended as the basis for a moisture reliability standard [4]. We see that the simple method of using average temperatures and humidities in Eq. (7) to compute AFs never overestimates the AFs, and can underestimate the AFs by 3x to 10x. Note, however, that for locations with lnAF > -0.4, that is, AF > 0.7, relative to 25/85, for Q = 0.9 eV, and C = 3 the errors are small. The same observations (not shown) are true for the indoor uncontrolled ambient, and the indoor controlled ambient. In the important case of the indoor controlled environment for thermal-only mechanisms (C = 0), this amounts to *all* locations.

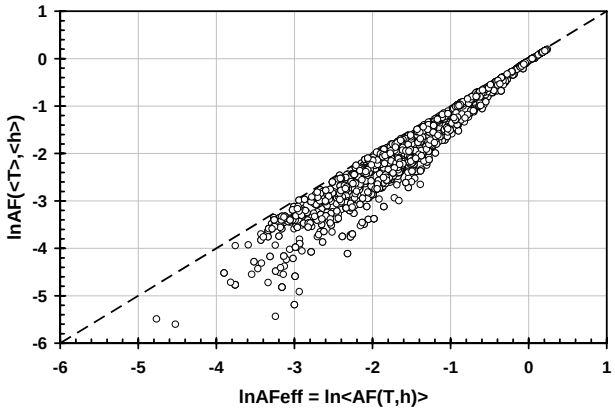

FIG. 10 AF AT TIME-AVERAGE TEMPERATURE AND RH (Y AXIS), VS AF AVERAGED OVER CORRELATED TEMPERATURE/RH PROFILES (AFEFF). FOR OUTDOOR ENVIRONMENT. NATURAL LOGS OF AFS RELATIVE TO 25/85 WITH Q = 0.9 EV, AND C = 3 ARE PLOTTED.

Distributions of AF were obtained for each of the use conditions for acceleration model parameters in the ranges $0 \le Q \le 1.2$ eV, and $0 \le C \le 4$, and for constant-in-time values of T_{rise} in the range $0 \le T_{rise} \le 10$ °C, except for the dashboard use condition for which only $T_{rise} = 0$ was considered. This was done by integrating AF over the time variation of T_{use}/h_{use} at each location. For the dashboard model, the parameters determined by model regression at 21 locations were used to compute AF relative to 25 °C at 1111 locations, taking into account the time variation of the solar contribution to temperature at each location through θ_{sun}, and through F_{cloud} (from the NOAA database) which varied from location to location. In Fig. 11 we show an example of the AF distributions obtained for the dashboard model. Similar sets of distributions were obtained for the outdoor ambient, the indoor uncontrolled ambient, and the indoor controlled ambient. For each distribution, values of AF at the standard 50th, 60th, 90th, 95th, and 99th percentiles were extracted. These are given in Table I. For all except the dashboard model, the analysis was also done, but results aren't shown, for $T_{rise} > 0$.

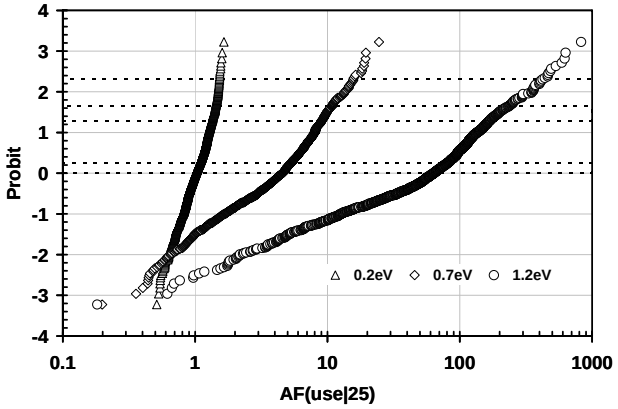

FIG. 11 DASHBOARD MODEL AF DISTRIBUTIONS, RELATIVE TO 25 C FOR THREE ACTIVATION ENERGIES. PERCENTILES WERE EXTRACTED AT 50, 60, 90, 95, AND 99 PERCENTILES (HORIZONTAL DASHED LINES).

TABLE I ACCELERATION FACTORS RELATIVE TO 25/85 AT VARIOUS PERCENTILES OF THE AF DISTRIBUTIONS FOR OUTDOOR, INDOOR UNCONTROLLED, INDOOR CONTROLLED, AND DASHBOARD ENVIRONMENTS, FOR $T_{RISE} = 0$. THE LAST 3 ROWS COME FROM FIG. 12.

	Reliability Model		Percentile of AF Distribution				
	Q (eV)	C	50	60	90	95	99
Outdoor	0.20	0	0.721	0.766	0.971	1.044	1.080
	0.70	0	0.410	0.487	0.983	1.202	1.376
	1.20	0	0.297	0.371	1.058	1.430	2.062
	0.20	2	0.497	0.526	0.698	0.792	0.986
	0.70	2	0.239	0.277	0.619	0.785	1.119
	1.20	2	0.152	0.202	0.649	0.886	1.266
	0.20	4	0.394	0.435	0.614	0.694	0.960
	0.70	4	0.179	0.212	0.497	0.665	1.104
	1.20	4	0.103	0.134	0.482	0.718	1.250
Indoor Uncontrolled	0.20	0	0.864	0.899	1.061	1.087	1.112
	0.70	0	0.662	0.744	1.268	1.356	1.461
	1.20	0	0.572	0.686	1.563	1.720	2.052
	0.20	2	0.262	0.291	0.544	0.691	0.854
	0.70	2	0.206	0.248	0.618	0.836	1.067
	1.20	2	0.188	0.234	0.729	1.025	1.342
	0.20	4	0.108	0.129	0.341	0.492	0.715
	0.70	4	0.087	0.114	0.387	0.595	0.894
	1.20	4	0.077	0.107	0.459	0.724	1.116
Indoor Controlled at 22.2 C	0.20	0	0.959	0.968	1.063	1.085	1.106
	0.70	0	0.873	0.909	1.260	1.352	1.465
	1.20	0	0.808	0.875	1.521	1.710	2.006
	0.20	2	0.367	0.389	0.577	0.712	0.884
	0.70	2	0.331	0.358	0.648	0.849	1.084
	1.20	2	0.302	0.333	0.774	1.026	1.354
	0.20	4	0.169	0.188	0.375	0.504	0.770
	0.70	4	0.153	0.174	0.424	0.625	0.944
	1.20	4	0.140	0.164	0.495	0.739	1.152
Dash-board	0.20	0	1.009	1.081	1.338	1.425	1.530
	0.70	0	4.564	5.371	9.009	10.820	15.792
	1.20	0	63.503	80.952	166.972	233.589	438.116

It is useful to represent the results of this study by a regression model for each percentile, p, of the AF distributions for each of the use condition models, u. For each use condition and percentile in Table I, the natural logarithm of the AF was fitted to a polynomial in Q and C. A linear fit was not sufficient to represent the results, but a biquadratic fit was adequate over the range of interest. We also

explored the sensitivity to a constant-in-time T_{rise} in the range $0 \le T_{rise} \le 10$ ºC, except for the dashboard model. The fitted equation is

$$\begin{aligned}\ln AF(u \mid ref; p) &= a(Q - wC)T_{rise} \\ &+ \sum_{\substack{m=0,2 \\ n=0,2}} b_{mn}(u,p) Q^m C^n \\ &+ \frac{Q}{k_B}\left(\frac{1}{273+T_{ref}} - \frac{1}{273+25}\right) \\ &+ C\left(\ln(0.85) - \ln h_{ref}\right)\end{aligned} \tag{18}$$

where a, w, and b_{mn} are regression parameters.

The first term in Eq. (18) represents the effect of T_{rise}. We found that this term does not depend on the specific model of environment (u), or on the percentile of the population (p). For the outdoor, indoor uncontrolled, and indoor controlled environments the regression gave a = 0.1276, and w = 0.45 eV. The second term involving b_{mn} is a regression fit to accelerations obtained by integrating the various climates over the Arrhenius/Peck temperature/relative humidity acceleration model, using a reference condition of 25/85. Note that b_{00} = 0 for all u and p. Values of b_{mn} are given in Table II. The final terms in Eq. (18) translate the reference condition from 25/85 at which the b_{mn} coefficients were determined, to any reference condition, T_{ref}/h_{ref}.

It is interesting to compare Eq. (18) with Eq. (10). If T_{rise}, T_{air}, and h_{air} (aka x, y, and z) are constant in time, then

$$a = \frac{1}{k_B T_{air}^2} \quad b_{10} = -\frac{1}{k_B T_{air}} \quad b_{01} = \ln h_{air} \quad w = W = 0.42\,\text{eV}$$

$$b_{00} = b_{02} = b_{11} = b_{12} = b_{20} = b_{21} = b_{22} = 0$$

The values of b_{mn} in Table II deviate from these values because of the effect of time variation of T_{air}. The fitted value of a corresponds to T_{air} = 28.6 ºC.

TABLE II. REGRESSION COEFFICIENTS B_{MN} FOR EQ. (18). $B_{00} = 0$.

		b01	b02	b10	b11	b12	b20	b21	b22
Outdoor	50	-0.1936	0.0134	-1.6309	-0.1991	0.0327	0.5314	0.0216	-0.0130
	60	-0.1655	0.0123	-1.3199	-0.4253	0.0694	0.4412	0.2152	-0.0474
	90	-0.0766	0.0090	-0.0576	-0.4375	0.0474	0.1247	0.2301	-0.0302
	95	-0.0530	0.0075	0.2124	-0.2363	0.0099	0.0754	0.0968	-0.0016
	99	-0.0141	0.0062	0.3823	-0.1845	0.0208	0.1099	-0.0031	0.0037
Indoor Uncontrolled	50	-0.6699	0.0350	-0.7871	-0.0014	0.0143	0.2680	0.0225	-0.0123
	60	-0.6295	0.0337	-0.5716	-0.0139	0.0078	0.2040	0.0234	-0.0038
	90	-0.3786	0.0207	0.1853	-0.0938	0.0179	0.0834	0.0540	-0.0105
	95	-0.2634	0.0117	0.3950	-0.0440	0.0127	0.0339	0.0114	-0.0051
	99	-0.1362	0.0087	0.4883	-0.0666	0.0117	0.0693	-0.0168	0.0009
Indoor Controlled at 22.2 C	50	-0.5273	0.0218	-0.2248	-0.0210	0.0039	0.0329	-0.0062	0.0020
	60	-0.5006	0.0218	-0.1673	-0.0320	0.0060	0.0466	-0.0092	0.0017
	90	-0.3219	0.0141	0.2445	-0.1593	0.0344	0.0561	0.0935	-0.0218
	95	-0.2611	0.0150	0.3835	0.0570	-0.0189	0.0531	-0.0771	0.0215
	99	-0.1345	0.0083	0.4654	-0.0488	0.0089	0.0752	-0.0259	0.0027
Dashboard	50			0.0974			2.8157		
	60			0.3984			2.7321		
	90			1.3877			2.4073		
	95			1.6467			2.4233		
	99			2.1453			2.4480		

Although the method described in this paper covers arbitrary models of time- and location-dependence of T_{rise} and T_{air}/h_{air}, the models of T_{rise} tend have a narrow device-specific scope, whereas models of T_{air}/h_{air} have a broad scope of application. It is convenient to have a method to compute the AF of a device without redoing the numerical integrations over T_{air}/h_{air} for every new T_{rise} model. It can be shown that in the usual case when the (time-varying) T_{rise} (ie. x) is sufficiently small compared to the time-average value of T_{air} (measured in ºK), then we can replace T_{air} (i.e. y) by its time average, $\langle y \rangle$ in the last term of Eq. (10). This gives

$$\begin{aligned}&AF(use \mid ref; x, y, z) \\ &\quad \cong \left(\frac{z}{h_{ref}}\right)^C \exp\left\{\frac{Q}{k_B}\left(\frac{1}{T_{ref}} - \frac{1}{y}\right)\right\} \exp\left\{\frac{(Q - WC)x}{k_B \langle y \rangle^2}\right\}\end{aligned} \tag{19}$$

When Eq. (19) is substituted into Eq. (5), the terms involving x factorize to produce a separately integrable T_{rise}-related acceleration factor which will multiply the AFs given in Table I or computed using Eq. (18) with coefficients from Table II (with T_{rise} = 0). Note that we also need to use the already-invoked "perfect time-uncorrelation" between T_{rise} and T_{air}. So we get

$$\begin{aligned}&AF_{eff}(use \text{ with } T_{rise} \text{ model} \mid ref) \\ &\quad \cong AF\left(use \text{ with } T_{rise} \text{ model} \mid \langle T_{air} \rangle\right) \\ &\qquad \times AF_{eff}\left(use \text{ with } T_{rise} = 0 \mid ref\right)\end{aligned}$$

where the T_{rise} device-specific AF is

$$\begin{aligned}&AF\left(use \text{ with } T_{rise} \text{ model} \mid \langle T_{air} \rangle\right) \\ &\quad = \int_0^\infty \kappa(x) \exp\left(\frac{(Q - WC)x}{k_B \langle T_{air} \rangle^2}\right) dx\end{aligned} \tag{20}$$

Eq. (20) is the T_{rise} time-PDF, $\kappa(x)$, integrated over an Arrhenius acceleration function, relative to $\langle T_{air} \rangle$, with activation energy $Q - WC$. The integral can be evaluated for any specific model of T_{rise} using the methods in the Appendix. This AF is then multiplied by the AF in Table I (or computed from Eq. (18) with T_{rise} = 0) to give the final AF relative to some reference condition T_{ref}/h_{ref}. We have performed exact calculations for time-varying T_{rise}, using the general form of the model derived in this paper, and have found the approximation to be quite accurate in most circumstances.

SUMMARY

We derived four models of temperature/humidity use conditions for which summary statistics are shown in Table III. Although these statistics are interesting, they should be used cautiously for reliability assessments. Reliability assessments require computation of acceleration factors by averaging over time-varying use conditions at each of many locations. We have described the theoretical formulation of the problem, and computational methods for doing this.

We noticed a simplification for the outdoor and indoor models for locations with $AF > 0.7$, relative to 25/85, In this case, only a small error relative to integration of the AF is incurred by using the time-

average temperature and time-average humidity in the standard Arrhenius/Peck acceleration model.

We have provided a convenient regression model, Eq. (18) for computing the AF at several standard percentiles of the location distributions as a function of Q and C (Arrhenius/Peck acceleration parameters), assuming a constant T_{rise}. We have shown a convenient extension of the method to arbitrary models of T_{rise}. This extension applies a multiplicative factor to the T_{air}/h_{air} AF at each of the locations, depending on an arbitrary model of T_{rise} at each location.

TABLE III SUMMARY STATISTICS OF MODELS.

	Outdoor	Indoor Uncontrolled	Indoor Controlled	Dashboard	Units
Grand average temperature. Location average of time-average temperature.	14.02	19.85	23.86	22.45	ºC
Location standard deviation of time-average temperatures.	6.26	4.18	1.68	8.07	ºC
Location average of time-standard deviations of temperatures.	8.06	5.27	1.93	19.12	ºC
Grand average relative humidity. Location average of time-average humidity.	0.71	0.48	0.52		0 ≤ h ≤ 1
Location standard deviation of time-average humidity of each location.	0.10	0.10	0.09		0 ≤ h ≤ 1
Location average of time-standard deviations of relative humidities.	0.12	0.11	0.11		0 ≤ h ≤ 1
Location correlation among time-average temperature and time-average humidity.	-0.12	0.71	0.44		-1 ≤ ρ ≤ 1

APPENDIX

Local Device Temperature Rise, T_{rise}

T_{rise} time variation can be represented by, for example, a multimodal time-PDF such as.

$$\kappa(x) = \frac{1}{\sqrt{2\pi}} \sum_{n=1}^{2} \frac{g_n}{\sqrt{T_{rise\_\mathrm{var}}(n)}} \exp\left\{ -\frac{(x - T_{rise\_mean}(n))^2}{2 \times T_{rise\_\mathrm{var}}(n)} \right\}. \quad \text{(A1)}$$

The parameters of this PDF will vary with location. For simplicity in the model calculations presented in this paper, we take T_{rise} to be constant in time at each location, although it may vary from location to location. That is

$$\kappa(x) = \delta\left(x - T_{rise}\right). \quad \text{(A2)}$$

where δ is a delta function.

Ambient Temperature, T_{air}

Uncontrolled Ambients: The distribution of daily average outdoor ambient temperatures for each of many locations in the world is well-represented by the PDF:

$$\lambda(y) = \frac{1}{\sqrt{2\pi}} \sum_{n=1}^{2} \frac{f_n}{\sqrt{T_{\mathrm{var}}(n)}} \exp\left\{ -\frac{(y - T_{mean}(n))^2}{2 \times T_{\mathrm{var}}(n)} \right\} \quad \text{(A3)}$$

The 5 parameters (note that $f_2 = 1 - f_1$) shown in bold (example shown in Figs. 1 and 3) are determined from NOAA and survey data for each of many locations [1]. For outdoor ambients, the two modes represent summer and winter seasons.

Controlled Ambients: Thermostatically set heating and cooling limits (or human avoidance of extremes) may be modeled by adding minimum and maximum temperatures, T_{min} (eg. heater thermostat setting) and T_{max} (eg. air-conditioning thermostat setting) with $T_{min} \leq T_{max}$ to the 5 parameters of the model in Eq. (A3). These additional parameters may also be different for each location.

Ambient Humidity, h_{air}

The humidity distribution corresponding to each value of T_{air} must fall in the range $0 \leq h_{air} \leq 1$. Variables constrained in this way are likely to be distributed according to a Beta distribution, and we have observed this. So we write the density function μ, describing the PDF of ambient humidity z for each ambient temperature y as

$$\mu(y,z) = \frac{\Gamma[\alpha(y) + \beta(y)]}{\Gamma[\alpha(y)] \cdot \Gamma[\beta(y)]} z^{\alpha(y)-1} (1-z)^{\beta(y)-1} \quad \text{(A4)}$$

where Γ is the Gamma function, and where we have made the T_{air} (aka y) - dependence of the α and β shape parameters explicit. This corresponds to the observation that the distribution of all the values of humidity which occur at a given value of T_{air} changes with that value.

The shape parameters, α and β, of the Beta distribution are related to the mean, m, and variance, v, of the distribution as follows:

$$\alpha(y) = m(y)\left\{ \frac{m(y) \cdot [1 - m(y)]}{v(y)} - 1 \right\} \quad \text{(A5a)}$$

$$\beta(y) = [1 - m(y)]\left(\frac{m(y) \cdot [1 - m(y)]}{v(y)} - 1 \right) \quad \text{(A5b)}$$

For each location, the mean and variance of the relative humidity as a function of T_{air} (aka y) in ºC was fitted to a quadratic between limits, determining the 8 parameters shown in bold (example given in Figs. 1 and 3 in the main text):

For $Trh_{min} \leq y \leq Trh_{max}$

$$m(y) = a\_m \times y^2 + b\_m \times y + c\_m \quad \text{(A6a)}$$

and

$$v(y) = a\_v \times y^2 + b\_v \times y + c\_v. \quad \text{(A6b)}$$

Note that y in Eqs. (A6a, b) is in °C, not °K. When y falls outside the range $Trh_{min} \leq y \leq Trh_{max}$, $m(y)$ and $v(y)$ are evaluated at the limiting values.

Computational Method

A semi analytical method for computing Eq. (5) is given by

$$AF_{eff}(use\,|\,ref) = \int_0^\infty dx\kappa(x)\left[\int_0^\infty dy\lambda(y)AF(x,y)\right]$$

$$\cong \frac{1}{\pi}\sum_{m=1}^{2}\sum_{n=1}^{2}\sum_{i=1}^{N}\sum_{j=1}^{N}\left\{\begin{array}{l} g_m f_n w_i w_j \times \\ AF\left(\begin{array}{l} T_{rise\_mean}(m) + x_i\sqrt{2T_{rise\_var}(m)}, \\ T_{mean}(n) + x_j\sqrt{2T_{var}(n)} \end{array}\right) \end{array}\right\} \quad \text{(A7)}$$

where (w_i, x_i, i = 1, N) are standard weights and sample points of the Gauss-Hermite quadrature, which are tabulated [8], where

$$AF(x,y) = \frac{1}{h_{ref}^C}\left[\frac{P_{sat}(y)}{P_{sat}(x+B(y))}\right]^C \times \exp\left[\begin{array}{l} \dfrac{Q}{k_B}\left(\dfrac{1}{T_{ref}} - \dfrac{1}{x+B(y)}\right) \\ +\ln\Gamma(\alpha(y)+\beta(y)) + \ln\Gamma(\alpha(y)+C) \\ -\ln\Gamma(\alpha(y)) - \ln\Gamma(\alpha(y)+\beta(y)+C) \end{array}\right]. \quad \text{(A8)}$$

where

$$B(y) = \begin{cases} T_{\min} & y < T_{\min} \\ y & T_{\min} \le y \le T_{\max} \\ T_{\max} & y > T_{\max} \end{cases}. \quad \text{(A9)}$$

Eq. (A7) is an optimal weighted sum over evaluation points of $AF(x,y)$. Values of 3 or 4 for N give numerical accuracy better than about 2%. Eq. (A8) takes advantage of an analytical result for the integration of the Peck acceleration model over the Beta parametric representation of the humidity PDF.

REFERENCES

[1] National Oceanic and Atmospheric Administration. http://www.noaa.com/. 5 CD-ROM volume collection of international surface weather observations. Hourly climatic data for approximately 1500 weather stations globally from 1997. http://www4.ncdc.noaa.gov/cgi-win/wwcgi.dll?wwAW~MP~CD/

[2] JEDEC Standard JESD94, "Application-Specific Qualification Using Knowledge Based Test Methodology," JEDEC Solid State Technology Association, January 2004.

[3] S. Peck, "Comprehensive Model for Humidity Testing Correlation," in Proc. 24th Ann. Int'l Reliability Physics Symposium, pp. 44-50 (1986).

[4] O. Hallberg and D. S. Peck, "Recent Humidity Accelerations, A Base for Testing Standards," Quality and Reliability Engineering International, Vol. 7 pp169-180 (1991).

[5] C. Glenn Shirley, "THB Reliability Models and Life Prediction for Intermittently-Powered Non-Hermetic Components," in Proc. 32nd Ann. Int'l Reliability Physics Symposium, pp. 72-77 (1994)

[6] Maxim/Dallas Semiconductor, Sunnyvale, CA, Part No. DS1922L.

[7] Gaylon S. Campbell, John M. Norman, An Introduction to Environmental Biophysics, Springer, New York, 1998, p. 174.

[8] M. Abramowitz, and I. A. Stegun, "Handbook of Mathematical Functions," Dover (1965), p924.